



SEISMIC UPGRADE OF FAULT CROSSING WATER PIPELINES USING LARGE DIAMETER EARTHQUAKE RESISTANT DUCTILE IRON PIPE

M. Hachem⁽¹⁾, R. Parra⁽²⁾, J. Lai⁽³⁾, A. Barnes⁽⁴⁾, A. Ambrosio-Meir⁽⁵⁾, D. Baune⁽⁶⁾, W. Chai⁽⁷⁾

⁽¹⁾ Mahmoud Hachem, PhD, SE, Principal, Earthquake Solutions, mahmoud@eqsols.com

⁽²⁾ Roger Parra, SE, Principal, Degenkolb Engineers, rparra@degenkolb.com

⁽³⁾ Jiun-Wei Lai, PhD, PE, Design Engineer, Degenkolb Engineers, jlai@degenkolb.com

⁽⁴⁾ Alex Barnes, PE, Project Engineer, Degenkolb Engineers, abarnes@degenkolb.com

⁽⁵⁾ Anthony Ambrosio-Meir, PE, Designer, Degenkolb Engineers, aambrosiomeir@degenkolb.com

⁽⁶⁾ Darren Baune, PE, Project Manager, Carollo Engineers, Inc., dbaune@carollo.com

⁽⁷⁾ Winston Chai, PE, Team Manager, Metropolitan Water District of Southern California, wchai@mwdh2o.com

Abstract

This paper presents the evaluation and retrofit of an existing 3.76-meter diameter welded steel water pipeline located at the Casa Loma Fault in Southern California. The Project will replace the existing pipeline with two 2.64-meter diameter earthquake resistant ductile iron pipes (ERDIP). The existing pipeline passes through a region that has 3.9-meter potential ground movement due to fault rupture and 0.8-meter seismic induced settlement that could cause significant damage to the existing pipelines. In order to reduce the risk of pipeline failure during a fault rupture, a series of conceptual seismic upgrade alternatives were studied with various mitigation strategies, including consideration of different pipe alignments, different backfill materials and pipelines with seismic resistant pipe joints. Because of high ground deformations, the preliminary analyses led to a design alternative that incorporates ERDIP with a soft backfill material to allow the pipelines to deform in multiple directions. This project developed an innovative ERDIP joint modeling concept in the finite element analysis program ABAQUS to simulate the joint deformation interaction along axial and rotational degrees of freedom, and combined with traditional soil-pipe interaction modeling approach to examine the pipeline performance. A full-scale test was conducted to verify design properties of ERDIP joint. During the final analysis phase, pipeline performance optimizations and sensitivity studies were performed to consider different fault crossing angles, fault crossing locations and ground movement scenarios to verify the seismic performance of the replacement pipelines.

Keywords: water pipeline, fault-crossing analysis, soil-pipe interaction, earthquake resistant ductile iron pipe



1. Introduction

This paper discusses the results of the numerical simulation performed for the seismic upgrade and replacement of an existing welded steel pipeline that crosses a major fault in California, and describes the numerical simulation used to evaluate the performance of the final design of the pipeline system. The owner of the pipeline is a regional water agency that owns and operates a complex water delivery system consisting of conveyance, distribution and treatment facilities.

The subject pipeline (designated as Casa Loma Siphon Barrel No. 1) is one of the large diameter pipelines that conveys potable water supply from a major aqueduct across the San Jacinto fault zone. The original pipeline was constructed in 1935 as a 3.75-m diameter concrete pipe. In 1968, approximately 100 meters of the concrete pipe was replaced with 3.75-m diameter steel pipe with sleeve-type couplings, because of cracks and significant leakage began to develop in the pipeline as a result of ground subsidence in the vicinity the fault crossing. Fig. 1 shows a plan view of the site.

The primary objectives of the Project are to retrofit the pipeline for the estimated Casa Loma Fault coseismic displacement, and non-tectonic ground subsidence, and significantly reduce the damage and post-earthquake recovery time.

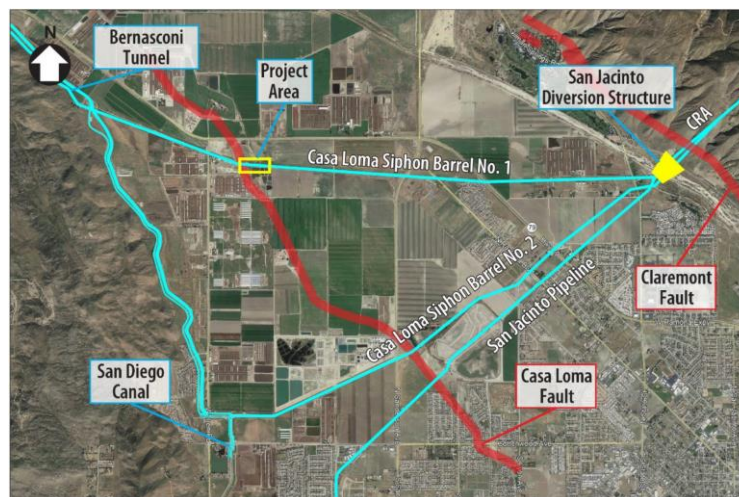


Fig. 1 – Casa Loma Siphon Barrel No. 1 Vicinity Map

2. Geotechnical & Geologic Investigations

The Casa Loma Fault is a main segment of the San Jacinto Fault Zone and is a right lateral strike slip fault, with a component of oblique normal downward displacement. In the recorded history since 1769, there have been 10 earthquakes with magnitudes greater than 6.0 within the San Jacinto fault system. The Casa Loma Siphon Barrel No. 1 is also subject to ground subsidence, likely due to groundwater pumping within the San Jacinto basin, near the Project location. The seismic and ground settlement design ground deformation values were recommended by the project geologist, based on an extensive geological investigation, including trenching and review of historical data, and a probabilistic seismic fault displacement hazard analysis which considered a deterministic and a probabilistic 2475-year events. The anticipated movement of the fault crossing is approximately 3.9 meters, which was controlled by the probabilistic event, with an average angle relative to the pipeline of 65 degrees, and the estimated non-tectonic vertical settlement is approximately 1-meter over 50 years. Multiple scenarios for representing the ground deformation along the pipeline were recommended. The four recommended scenarios account for the uncertainty in the location and orientation of the fault at the pipeline crossing, and for the uncertainty of the distribution and magnitude of the long-term ground settlement. Four modes of behavior were defined for both the fault rupture deformation distribution and the ground settlement deformation distribution as follows:



- Mode 1 – 100% of seismic fault movement concentrated anywhere in the primary zone
- Mode 2 – 85% of seismic fault movement anywhere in the primary zone and the remaining 15% anywhere in the secondary zone
- Mode 3 – Uniform distribution of 25% of the design ground settlement over the primary seismic zone, and a uniform distribution of the remaining 75% over the settlement zone
- Mode 4 – Uniform distribution within the primary fault zone and settlement zone

Fig. 2 shows the extents of the primary (red shading) and secondary (orange shading) fault zones, and of the zone of distributed non-tectonic settlement (blue shading). The combination of these modes of deformation resulted in four recommended scenarios which are intended to capture the range of possible deformation scenarios:

- Scenario 1 = Mode 1 + Mode 3
- Scenario 2 = Mode 1 + Mode 4
- Scenario 3 = Mode 2 + Mode 3
- Scenario 4 = Mode 2 + Mode 4

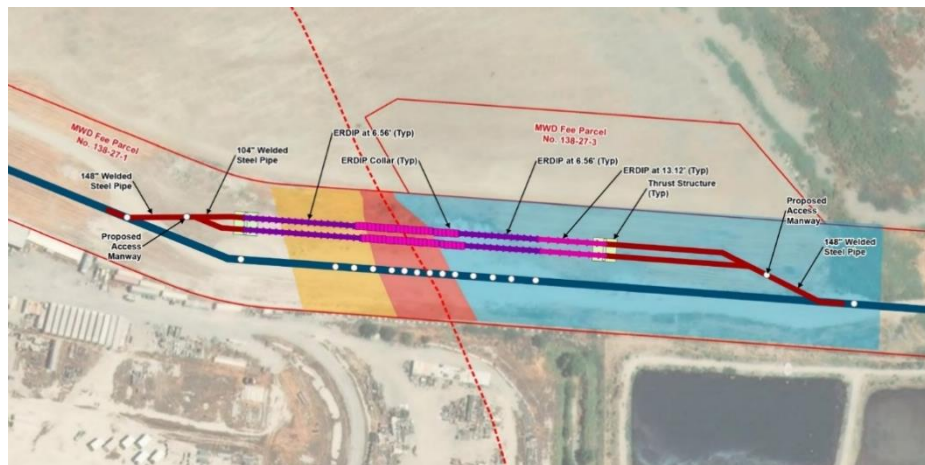


Fig. 2 – Plan View of Final Pipeline Design Layout

3. Alternatives Evaluation

Because of high ground deformations, the preliminary analyses led to a design alternative that incorporates Earthquake Resistant Ductile Iron Pipe (ERDIP) with a soft backfill material to allow the pipelines to deform in multiple directions. The alternatives analysis focused on pipeline systems that utilize ERDIP which is manufactured by the Kubota Corporation in Japan. The ERDIP dissipates large fault displacements by absorbing the fault displacement through axial expansion/compression and rotation within the pipe joints. The recommended alternative involves replacing approximately 330 meters of the existing 3.75-m diameter pipe using one of the following alternatives:

- **Alternative No. 1—Two 104-inch Barrels**
- Alternative No. 2—Three 84-inch Barrels
- Alternative No. 3—Displacement Vault

The alternative evaluation analysis resulted in the selection of Alternative No. 1 for the final design. The modeling and analysis then considered three different options, based on Alternative No. 1, which use different combinations of ERDIP joint types and spacings including regular joints, collar joints and long-collar joints, as shown in Fig. 3. Option 1 was found to be the most appropriate for achieving the project objectives.

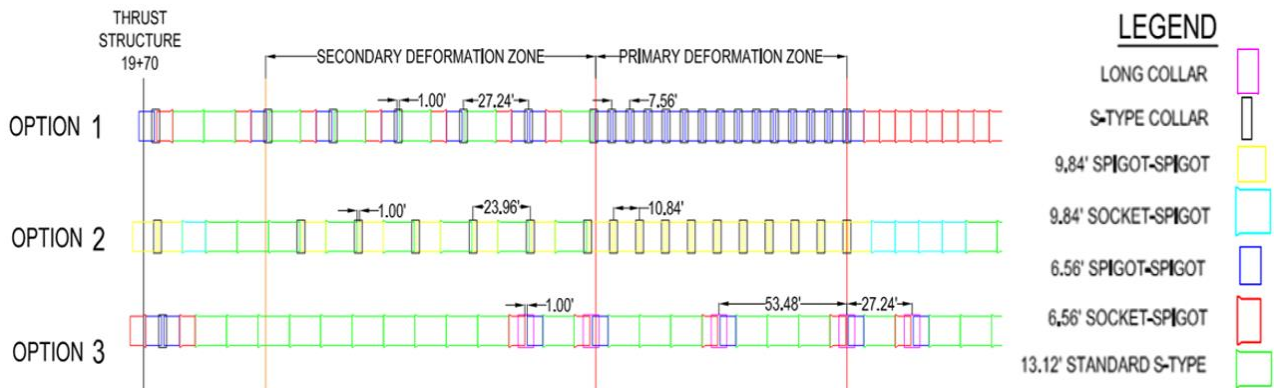


Fig. 3 – Three different options considered for the final design based on Alternative No. 1.

4. Finite Element Modeling

4.1 Geometry and Global Modeling

The pipeline system was modeled in the finite element software ABAQUS [1] using nonlinear frame elements that represent the ductile iron and steel pipe and nonlinear connector elements that represent the flexible ERDIP joints. Accurate modeling of the joint behavior is critical to predicting the response of the pipeline system. In addition to material nonlinearity, geometric nonlinearity was considered in the ABAQUS model in order to accurately predict the behavior of the pipeline under the large ground deformations. See Fig. 2 for the geometry.

The pipe segments between joints were modeled in ABAQUS using standard beam elements (PIPE31) with nonlinear material behavior. The beam elements were assigned pipe sections to represent the pipe section geometry. Pipe segments were modeled as disconnected elements that generally measure about 13-feet (or 6.5-ft for shorter segments) each and were connected using special nonlinear connector elements to represent the ERDIP joints.

4.2 Soil Modeling

Spring elements were used to model the native soil and backfill stiffness and strength in ABAQUS, which were assigned a set of representative spring properties to model the native soil and backfill behavior along the length of the pipe. The native soil properties recommended by the geotechnical engineer were based on field investigation and geotechnical testing performed on field samples. Three orthogonal nonlinear (bilinear) soil springs were used at each element node; each connected to a fixed node representing the ground. The directions of the springs were aligned with respect to the pipe element direction such that one spring was oriented parallel to the longitudinal axis of the pipe element representing friction between the pipe and the surrounding soil (t-x springs); one spring was perpendicular to the element representing lateral horizontal soil resistance (p-y springs); and the last spring was defined perpendicular to the element in a vertical plane representing bearing and uplift resistance (q-z spring). Fig. 4 illustrates the ABAQUS model spring representation.

Soil springs were modeled using nonlinear elastic-plastic springs with a very small post-yield stiffness that were active in both the negative and positive directions. The longitudinal (t-x) and horizontal/transverse (p-y) springs were modeled to have symmetric behavior in the positive and negative directions, while the vertical (q-z) springs were asymmetric with different behaviors in the up (uplift) and down (bearing) directions. This is due to the resistance of the soil-against-soil movement being substantially stiffer for bearing resistance compared to uplift resistance, especially for shallow pipe embedment depths. This approach of modeling the soil is consistent with standard soil modeling and follows recommendations for pipe-soil interaction in guidelines from the American Lifelines Alliance ([2], Fig. 4). Fig. 5 illustrates the force-displacement relationships used for the soil springs.

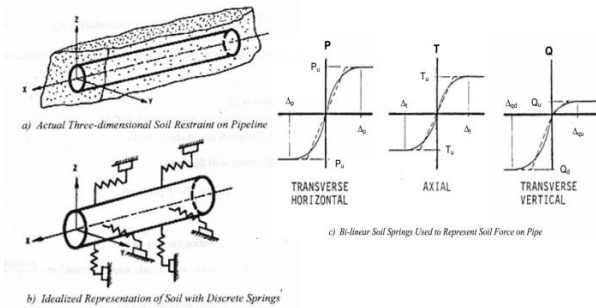


Fig. 4 – Idealized Representation of Soil-Pipe Interaction Springs [1]

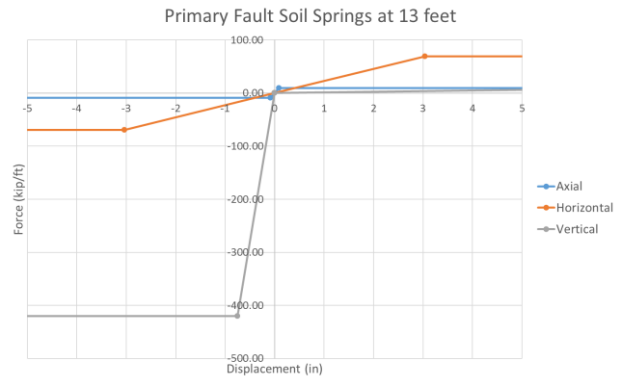


Fig. 5 – Nonlinear Force-displacement Relationships Used to Represent the Native Soil Springs

4.3 Expanded Polystyrene (EPS) Modeling

In the final design and corresponding ABAQUS analysis, expanded polystyrene (EPS) foam blocks were selected as backfill material within the primary fault zone. The EPS grade 22 Geo-foam was selected because the material’s low stiffness and strength help accommodate the large anticipated deformations at the fault crossing. Fig. 6 shows the EPS and native soil backfill configuration around the pipes along the primary fault zone.

Similar to the native soil modeling concept, the EPS foam blocks were modeled using nonlinear springs with an idealized trilinear behavior [3] and the typical EPS 22 foam block ASTM specification [4]. Since the EPS foam blocks are going to be placed at each side of the ERDIP within the primary fault zone, the horizontal (p-y) springs within that region were replaced by the trilinear springs with the EPS 22 force-deformation relationship, and the longitudinal (t-x) and the vertical (q-z) springs were modeled using the standard modeling approach with native soil properties. Fig. 7 shows the actual force-displacement relationship used for the EPS 22 trilinear springs. Note that the width of EPS block is assumed to be 10-ft on either side of the pipe (Fig. 6).

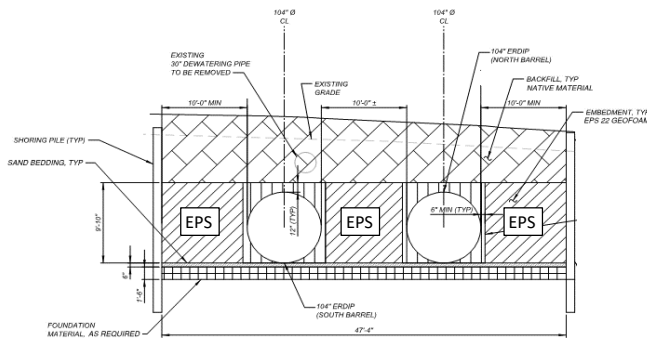


Fig. 6 – Section of Pipeline Trench using EPS Geofoam Blocks

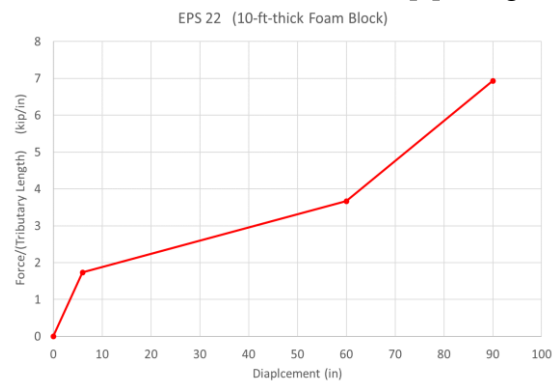


Fig. 7 – Nonlinear Force-displacement Relationship for EPS 22 Foam Blocks (Horizontal p-y Springs)

4.4 ERDIP Joint Modeling

The ERDIP joint models were developed and calibrated to match the joint axial and rotation response parameters provided by the ERDIP manufacturer [5]. In addition to the typical ERDIP joint (see Fig. 8 and Fig. 9), the ERDIP manufacturer provides a collar joint for use in high axial deformation areas (Figs. 10, 11).



The collar joint allows 5 times more axial deformation and twice the rotation deformation of a regular ERDIP joint. In general, the collar joint consists of an oversized and thickened short pipe segment with ERDIP joint on both sides, which allows for more sliding range, as well as a total rotation equal to the sum of rotations of the two joints at the two ends of the collar.

The ERDIP joints exhibit highly nonlinear behavior in the axial direction and in rotation about the two major bending axes (Fig. 12), while the response in shear is linear. As shown in Fig. 12, the force-deformation response of the joint in axial and bending is characterized by an initial slipping phase and finally by a locking phase exhibiting a steep increase in stiffness as the joint mechanism reaches its deformation capacity and locks. After locking, the joint has some additional capacity before the ultimate force/deformation capacity is reached. The steep increase in stiffness is a beneficial feature since the development of additional force allows for the redistribution of additional demands to neighboring joints that have not yet reached their limiting deformations, and allows a chain-like progression of slipping and rotation of successive joints, which mobilizes additional deformation capacity and enables the pipeline to resist larger deformations.

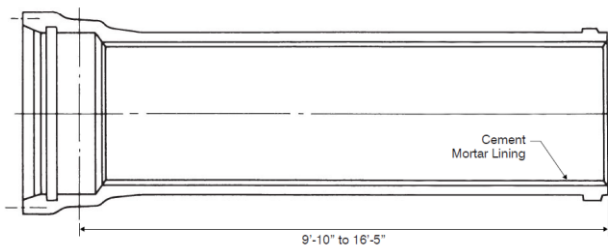


Fig. 8 – ERDIP Pipe

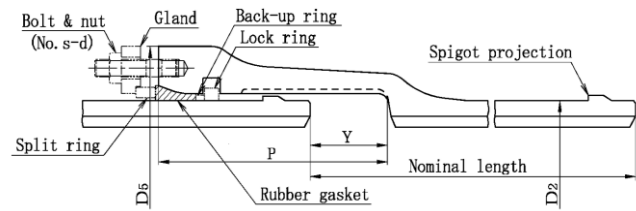


Fig. 9 – ERDIP Joint Detail

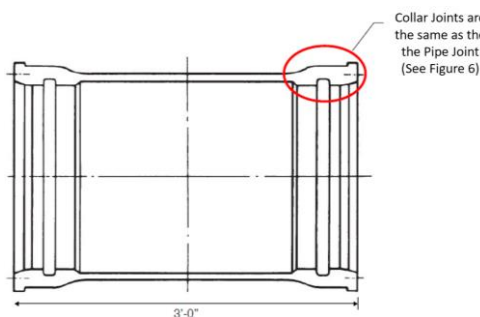


Fig. 10 – Pipe Collar Joint Section

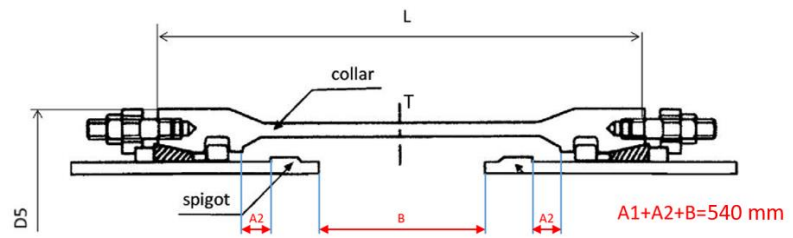


Fig. 11 – Pipe Collar Joint Detail

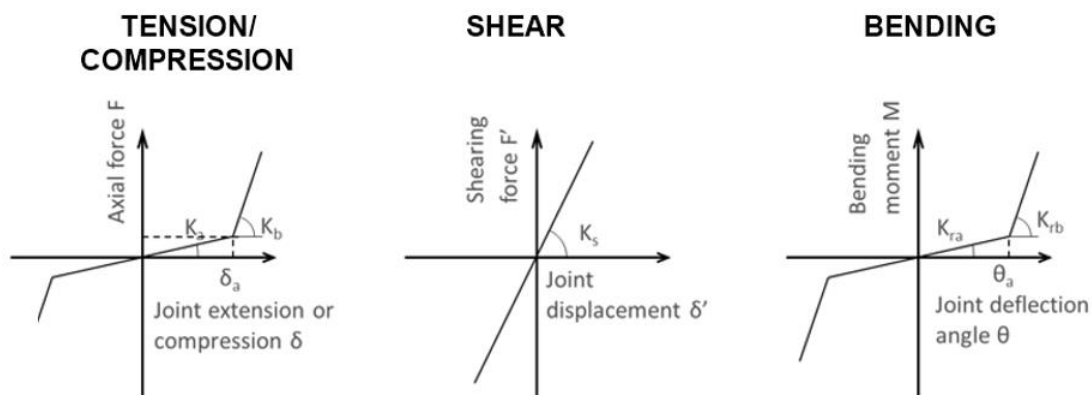


Fig. 12 – Updated Behavior Characteristics of ERDIP Pipe Joints and Collars [5]

The ERDIP joints and collars are characterized with deformation capability in compression and tension as well as rotation. Given the configuration of the joints, the axial and rotational deformation capacities are not



independent and are in-fact related to each other. Since the joints rely on the same locking mechanism for providing axial and rotational deformation capacities, it is then expected that there would be coupling between the axial and rotational deformation capacities. The joint cannot simultaneously be pushed to its full axial and full rotational capacities. This interaction between axial and rotational deformation limits can be estimated using a simple kinematic (geometric) calculation taking into account the joint dimensions and deformation capacity, and different interaction envelopes may be constructed for different types of joints

It is common practice to model ERDIP joints to have independent response in the two primary bending directions, resulting in a stronger section when loaded in both directions simultaneously. However, this is not exactly accurate since, in reality, the circular geometry of the joint means that it has the same bending and rotational capacity along any direction of a 360-degree range. Furthermore, it is common to neglect the interaction between rotation and axial response, which can lead to an inaccurate estimate of the joint's moment demand-to-capacity ratio. One way of estimating the effect of interaction and avoid underestimating demand, is to check for interaction during the post-processing of the results by simply combining the peak rotations and bending moments in the two major directions along the diagonal, as a way to estimate the peak resultant rotation and moment. However, this method overestimates the maximum resultant rotations, and can result in unrealistically high bending moment values.

In order to avoid these shortcomings, we developed a model that directly simulates the interaction between the moment in two directions and the axial force (PMM) for a more accurate simulation of response. The nonlinear behavior of the ERDIP joints was modeled using ABAQUS Connector elements. The Connector elements are able to represent the forces that arise due to the relative deformations between two connected joints, for all degrees of freedom, including translational and rotational. The Connector elements were configured to replicate the behavior of the joints in the axial direction (tension/compression), bending along two orthogonal axes, shear behavior in two orthogonal directions, as well as torsion. The response in each of the six degrees of freedom was modeled consistent with recommendations and published information from the manufacturer. A linear elastic behavior was assumed for the two shear directions in the joint, while nonlinear behavior was assumed in the remaining four modes of deformation.

4.5 Modeling Joint Interaction Behavior in ABAQUS

The conventional method of modeling ERDIP joints, which is generally recommended by the pipe manufacturer, assumes uncoupled behavior in the axial and two rotational degrees of freedom, and cannot predict interaction between those directions (e.g. Fig. 13). In order to overcome these limitations, we developed a novel modeling technique to simulate the effect of the triaxial interaction by using multiple connector elements at each joint with spring connectors distributed around the perimeter of the pipe section. The perimeter nodes are constrained to the center node using a rigid-body constraint in ABAQUS, which forces the 9 nodes to translate and rotate together as a rigid body.

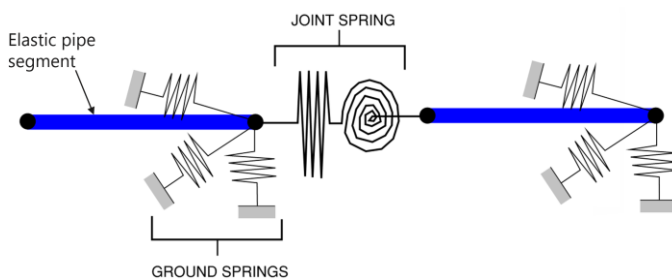


Fig. 13 – Conventional method for modeling ERDIP joints which does not capture Moment-Moment and Axial-Moment interactions

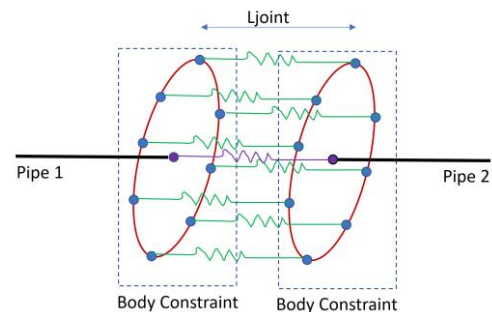


Fig. 14 – ABAQUS Spring model for simulating the triaxial interaction of the ERDIP regular joint

The perimeter springs undergo deformations under both axial extension/contraction and bi-axial rotation, which couples all three deformations. If rotations are applied along two axes instead of one, the joint



will lock earlier (with a smaller rotation value along each axis) than if loaded along one axis only. Similarly, applying axial deformation might lead the joint to lock earlier in rotation (at a smaller rotation value), effectively resulting in a reduced deformation capacity due to interaction. The perimeter springs were assigned a nonlinear behavior that is similar to that of the axial behavior of the joint, divided by the number of the springs such that the sum of the stiffness of all perimeter springs is equal to the overall axial stiffness.

Since the springs are distributed around the perimeter, they also contribute to the bending response of the joint, and hence they determine both the axial and bending behavior of the joint, and also provide full triaxial coupling between the axial behavior and rotational behaviors in two orthogonal directions. In addition to the perimeter springs, additional springs were added along the centerline of the joint that represent the linear shear and torsional behavior of the joint. As a result, the perimeter springs provide stiffness in axial and rotational behavior, while the center spring provides stiffness in shear and torsion. This technique resulted in a reliable simulation of the idealized circular interaction surface for the bending response as well as the full triaxial interaction. It was found that using eight (8) perimeter springs along the circumference of the pipe, at 45° spacing, provided sufficient accuracy to represent the coupled behavior of the joints. Fig. 14 is a graphical representation of the improved joint model used to model the ERDIP regular joint.

Since a collar is effectively an assembly of two regular pipe joints with a sliding pipe segment in between that allows additional axial/sliding deformation, it was possible to re-use the simple joint model to build the more complex collar model. The collar model was constructed by using two instances of the simple joint models (one at each end) connected by a sliding spring representing the additional sliding capacity of the collar joint.

4.6 Calibration of Joint Model to Test Data

In the process of converting the uncoupled model into the coupled spring model, we judged the rotational response of the joints to be more critical than the axial response, and we focused on matching the moment-rotation response as a higher priority. We modified the axial springs by applying modifiers to the hardening stiffness and onset of locking displacement. When the model is evaluated with the modified axial spring properties, the resulting moment-rotation response shows almost a perfect match with the recommended rotation spring properties. However, the modeled axial locking stiffness of the ERDIP joints is smaller than that recommended by the manufacturer. In order to verify that this difference in stiffness does not affect the accuracy of the analysis, we conducted a separate analysis using a modified joint model with a substantially higher axial stiffness. As a result of this study, we found that the axial stiffness has a very limited effect on the predicted pipeline response to the design ground deformations, and that the results of the proposed model are valid.

The project also included the successful testing of two full-scale 2.6-meter diameter ERDIP joints under monotonically increasing deformation, which verified the joint's ability to go beyond its design rotation, and was used to perform final calibration of the joint model.

4.7 Interaction Behavior of Calibrated ERDIP Joint Model

We analyzed the joint model by imposing pure axial or rotation deformation and measuring the resulting force or moment. We also applied various combinations (ratios) of axial and rotational deformations and measured the resulting force and moment. We then tracked the results to determine the failure point for each loading case (based on ratio of axial to rotation deformations). We defined failure as the first instance when one of the perimeter springs exceeds the axial deformation capacity (0.086m) or when the total force in the joint exceeds 7,800 kN, which is the axial force limit recommended by the manufacturer. The axial and rotational deformation interaction plots are shown in Fig. 15 and Fig. 16 for the regular joint and collar joint, respectively, and show excellent agreement with the interaction envelopes recommended by the manufacturer. Note that the model accurately predicts the force and deformation capacities of the joints.

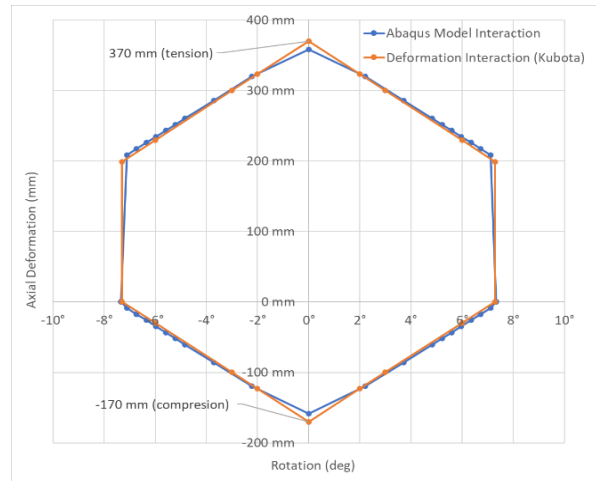
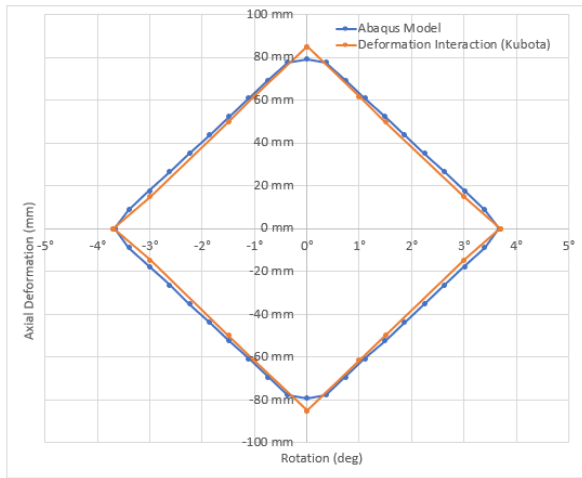


Fig. 15 – Axial/Rotation deformation interaction of ERDIP Joint ABAQUS model compared to recommendation from the manufacturer.

Fig. 16 – Axial/Rotation deformation interaction of the ERDIP Collar Joint ABAQUS model compared to recommendation from the manufacturer.

5. Analysis Results

In the final design analysis, a series of ABAQUS runs were performed based on multiple scenarios (see Section 2 for detail), fault crossing angles and fault crossing locations that represent the ground deformation along the pipeline for the final pipeline design layout in Fig. 2. Since the fault can rupture anywhere along the primary and secondary fault zones and since the angle of faulting can vary, three fault crossing angles and three fault crossing locations in both fault zones along with four ground movement scenarios were considered in the load case combinations. Considering all possible primary and secondary fault locations and settlement load cases for the four possible scenarios, we selected a total of 80 load cases to be applied in ABAQUS for the final analysis.

The pipeline global response and the ERDIP joint response are presented below under one of the controlling load cases for Scenario 3. This case represents ground movement with two fault crossings, one at the east boundary of the primary fault zone (0-m from the east primary zone edge) and the other at the west boundary of the secondary fault zone (42-m from the east secondary zone edge), the fault crossing angle is 75 degrees between the fault(s) and pipeline, and assuming the primary and secondary fault ruptures are parallel.

Fig. 17 presents the deformation interaction diagrams of S-type and collar joints for every joint between the thrust structures. Each red dot shown on the plots represents the axial and rotational deformations of a joint at particular station location.

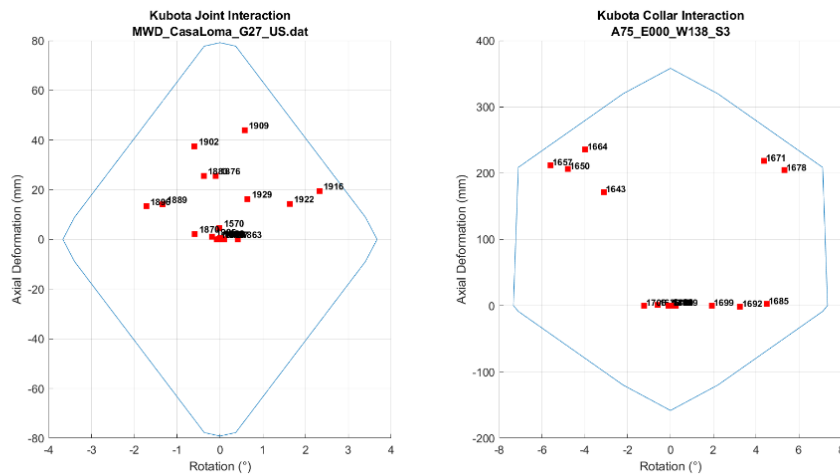


Fig. 17 – S-type Joint and Collar Joint Deformation Interaction Diagram



The ERDIP joint deformation limit considering interaction for each type of joint is plotted in solid blue line. From the interaction diagram, it is clear that all ERDIP joints are deformed within the limit under this load case, and the joints near the fault crossing regions generally have larger axial deformation as well as joint rotation as expected. This can be seen clearly in Fig. 18 that shows the distribution of joint axial deformation and joint rotation along the length of the pipeline.

Fig. 19 shows the distribution of axial force (tensile) and the bi-directional bending moments within the joints over the pipeline alignment. All joint force demands are less than the manufacturer’s allowable limits. Typical peak force and peak bending moments occur near the fault crossing.

The peak soil spring and EPS spring deformations are concentrated near the fault crossing region as shown in Fig. 20, which shows that the EPS foam block maximum compression strain is less than 0.5 (i.e. 50% compressive deformation).

Fig. 21 shows the beam stress along the pipeline and the deformed shape in the horizontal plane under the target ground deformation, the maximum stress along the pipe is around 3.6 ksi (24.8 MPa), which is very low.

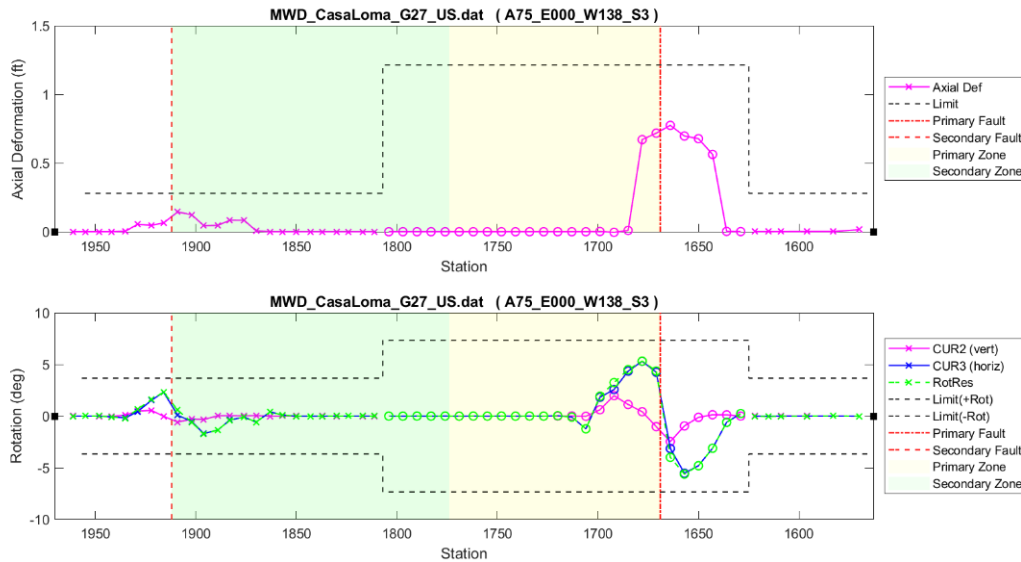


Fig. 18 – Joint Axial Deformation and Rotation Along the Pipe Alignment

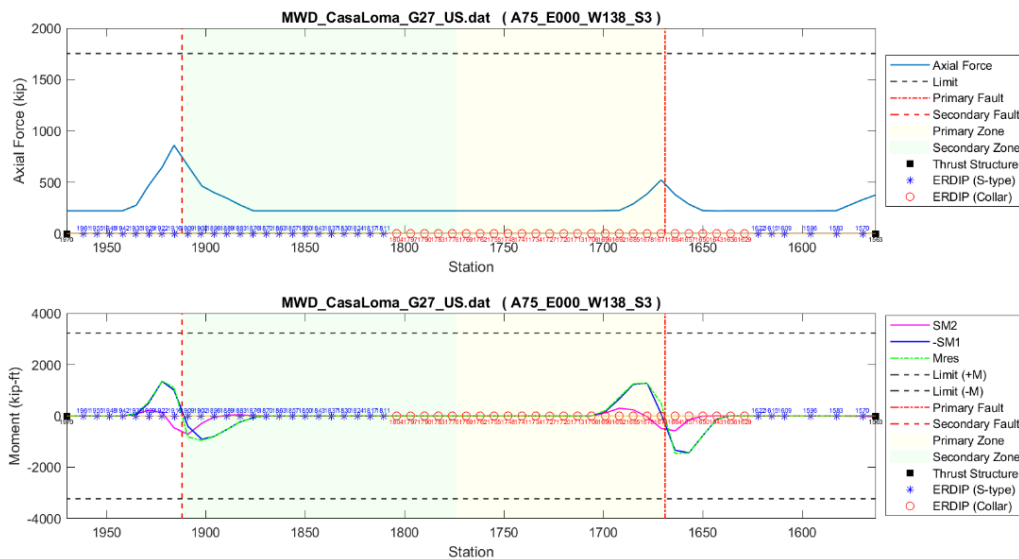


Fig. 19 – Axial Force and Bending Moment Along the Pipe Alignment

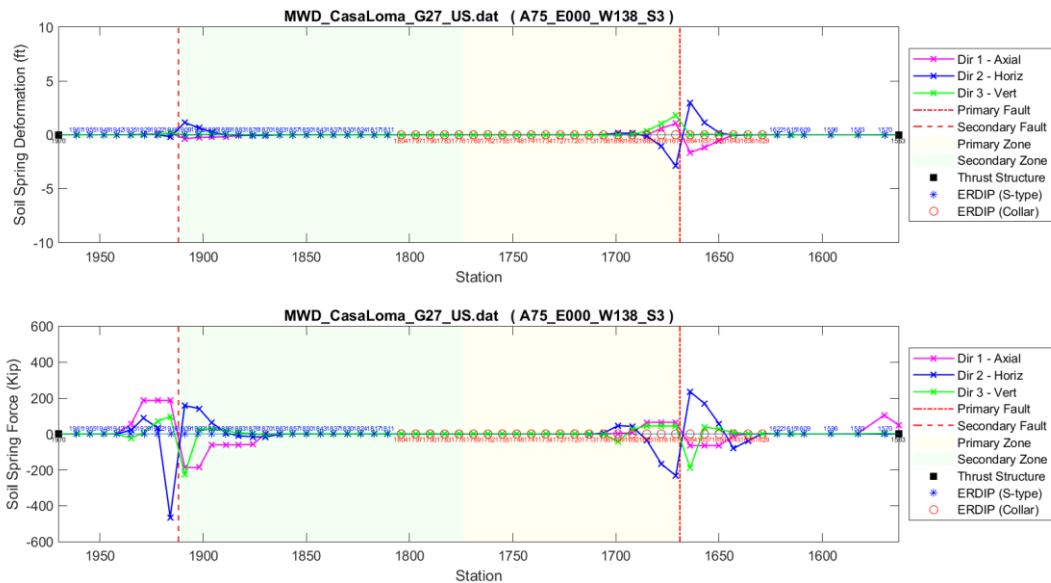


Fig. 20 – Soil and EPS Spring Deformation and Spring Force Along the Pipe Alignment

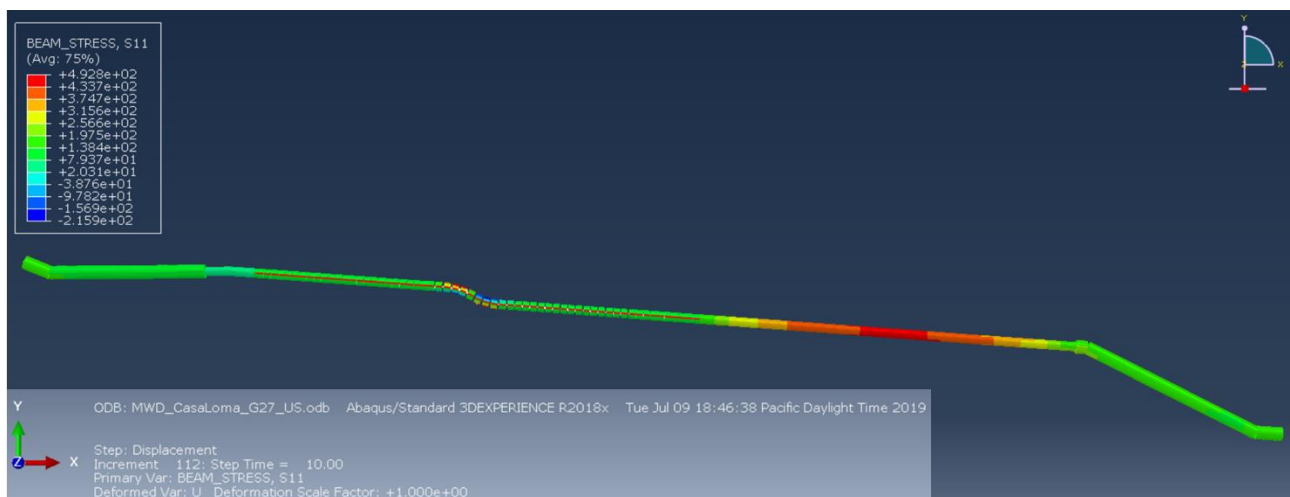


Fig. 21 – Deformed shape of the ABAQUS model and the longitudinal beam stresses along pipe alignment (unit: kip/ft²)

6. Recommended Final Design

Based on the results from the optimization studies, and considering the initial cost estimates for different design options, the most feasible ERDIP joint configuration that met the design criteria was selected, and a complete parametric study was then performed on the final design, which is shown in Fig. 2.

7. Conclusion

This paper discussed the global behavior of the proposed Replacement of Casa Loma Siphon Barrel No. 1 crossing the Casa Loma Fault zone. The parametric analysis studies performed using ABAQUS show that the proposed ERDIP joint configuration meets the design criteria under the provided ground movement scenarios. The axial/rotation deformation interaction diagrams developed during this study show that the ERDIP joint deformations are within the allowable limits provided by the manufacturer and no significant joint locking



behavior is observed in the parametric studies and the joint force demands are all less than the manufacturer's allowable limits.

A novel ERDIP joint PMM interaction model was developed in this project, and it was used to successfully model the complex behavior of the joints as they are subjected to a complex combination of translational and rotational deformations and forces. The model can accurately model the deformation and force interaction of the joint under demands in multiple degrees of freedom, allowing the demands on the joints to be evaluated accurately, and without the need to apply extra-conservatism in order to meet the design criteria.

The project also included the successful testing of two full-scale 2.6-meter diameter ERDIP joints under monotonically increasing deformation, which verified the joint's ability to go beyond its design rotation, and was used to perform final calibration of the joint model.

The sensitivity studies on the backfill materials show that the strength and stiffness of the backfill material has a significant effect on the ERDIP joint behavior. In general, softer backfill material will help spread out the ERDIP joint deformation in the areas of large displacement near the fault crossing. This helps in distributing deformations among a larger number of ERDIP joints and also reduces the joint force demands. The final design uses EPS 22 Geofoam blocks within the primary fault zone to improve joint deformation redistribution, and the EPS Geofoam material was shown to significantly improve the performance of the pipeline by providing a backfill with reduced stiffness that allow the pipeline to deform more freely, compared to native soil, when subjected to fault-induced ground deformations.

Project Team

The following summarizes the Project team members and key roles.

- Metropolitan Water District of Southern California is the owner of the pipeline.
- Carollo Engineers, Inc. served as the prime consultant and led the project team during the planning and final design phases.
- Degenkolb Engineers led the numerical simulations and analyses described in this paper.
- Lettis Consultants International, Inc. led the geologic investigations including the seismic hazard analysis, fault mapping, and fault displacement estimates.
- Hushmand and Associates led the geotechnical investigations.
- JDH Corrosion Consultants led the design of the cathodic protection facilities.

9. References

- [1] ABAQUS (2018), ABAQUS 6.20 Documentation, Dassault Systèmes, Providence, RI, USA.
- [2] ALA 2001. Guidelines for the Design of Buried Steel Pipe, American Lifelines Alliance (ALA) dated July 2001 (with 2005 Addenda).
- [3] Castiglioni, A., Castellani, L., Cuder, G. and Comba, S., (2017) Relevant Materials Parameters in Cushing for EPS Foams, Colloids and Surfaces A: Physicochemical and Engineering Aspects, Volume 534, pp.71-77.
- [4] ASTM D6817-15, 2017. Standard Specification for Rigid Cellular Polystyrene Geofoam.
- [5] Kubota, 2019. Technical Specification on Earthquake Resistant Ductile Iron Pipes prepared by Kubota Corporation.